Applied Catalysis B: Environmental 128 (2012) 171–178

Contents lists available at SciVerse ScienceDirect

Applied Catalysis B: Environmental

journal homepage: www.elsevier.com/locate/apcatb

Characterization of a new photocatalytic textile for formaldehyde removal from indoor air

Pierre-Alexandre Bourgeois[a], Eric Puzenat[a], Laure Peruchon[b], France Simonet[a], Delphine Chevalier[b], Emmanuel Deflin[b], Cédric Brochier[b], Chantal Guillard[a,*]

[a] IRCELYON, UMR 5256 CNRS-Université Lyon-1, 2 Av Albert Einstein, 69626 Villeurbanne-Cedex, France
[b] Brochier Technologies, 90 Av Frédéric Faÿs, 69100 Villeurbanne, France

ARTICLE INFO

Article history:
Available online 3 May 2012

This article is dedicated to our friend and colleague Jean-Marie Herrmann who devoted his research to the heterogeneous photocatalysis.

Keywords:
Photocatalysis
Lighted textile
Optical fiber
VOC
Irradiance modelling

ABSTRACT

The treatment of volatile organic compounds (VOCs) from different sources (industrial process, human activity, release of pollutants by materials, etc) in confined areas is a major challenge to prevent human health issues. Actually, one stays around 80% of a day in closed areas. The photocatalytic process is now recognized as an efficient method to remove organic pollutants present in gaseous phase. However, there are still some drawbacks with current reactors as for example lightutilization limitations due to absorption and/or scattering by the reaction medium or as restricted processing capacities due to mass transport limitations. The solution proposed in this work lies in the use of a lighted textile with optical fibers. The polymer optical fibers are treated to allow a radial leak of light through several dotted lights, allowing the carrying and the supply of UV light onto the overall textile area. Once coated using a suspension of TiO_2, the textile becomes a photocatalytic materials for which UV light is carried into the bulk of the photocatalytic bed. The modifications of the fibers surface have been characterized by ESEM. The topology was characterized by optical microscopy and the radiant flux was measured by radiometry. The characteristics of the coating such as the photocatalyst content, its location and its adherence have been studied to understand the coating properties. The photocatalytic efficiency of samples coated with TiO_2 was measured using formaldehyde as model molecule. The results obtained with a such new textile are very encouraging because this innovation allows to imagine a three dimensional light sources irradiate photocatalytic bed either its surface than its bulk. New perspectives in photocatalytic process are so opened.

1. Introduction

The quality of indoor air is crucial for human health, actually, the developed country populations spend more than 80% of their time in closed areas [1]. But, indoor air suffers different ways for the pollution sources: outside sources [2], human activities and release of pollutants by materials [3–5]. The photocatalytic process is more and more used to remove volatile organic compounds (VOCs), especially from indoor air treatment [6,7]. The interest of photocatalysis grows up for the industrial applications like indoor air treatment because it has several advantages as being efficient at room temperature, its low cost and its harmlessness.

However, photocatalytic processes need the combination of the photocatalyst, the pollutant and the light. Actually, the photocatalyst has to be activated by irradiation with UV light and the pollutant needs to be adsorbed on the surface of the photocatalyst to be degraded [8–10].

To optimize the lighting of the photocatalyst, different reactors have been developed during the last decade [11,12]. These ones used powder or supported TiO_2 but were always lighted with an external lamp [13,14]. However, there are some drawbacks with these current reactors as for example lightutilization limitations due to absorption and/or scattering by the reaction medium or as restricted processing capacities due to mass transport limitations. The use of optical fibers as support of photocatalyst was firstly proposed by Ollis and Marinangeli in 1977 and 1980 [15,16]. But the first experimental study with optical fibers was presented in 1994 for the water treatment of 4-chlorophenol by Hofstadler et al. [17]. Since 2001, more and more works using optical fibers as support of photocatalyst and different reactors were proposed for the air and water treatment [11,12,18–20]. In particular, one of us began the study of optical fibers coating with TiO_2 from 2001 with the Ph.D. A. Danion [20–23] showing the effect of fiber diameter, of TiO_2 thickness and the length of coating. The authors also optimize the photocatalytic optical fibers using experimental design and study

* Corresponding author. Tel.: +04 72 44 53 16; fax: +04 72 44 53 99.
E-mail addresses: pabbourgeois@gmail.com (P.-A. Bourgeois), chantal.guillard@ircelyon.univ-lyon1.fr (C. Guillard).

0926-3373/$ – see front matter © 2012 Elsevier B.V. All rights reserved.
http://dx.doi.org/10.1016/j.apcatb.2012.03.033

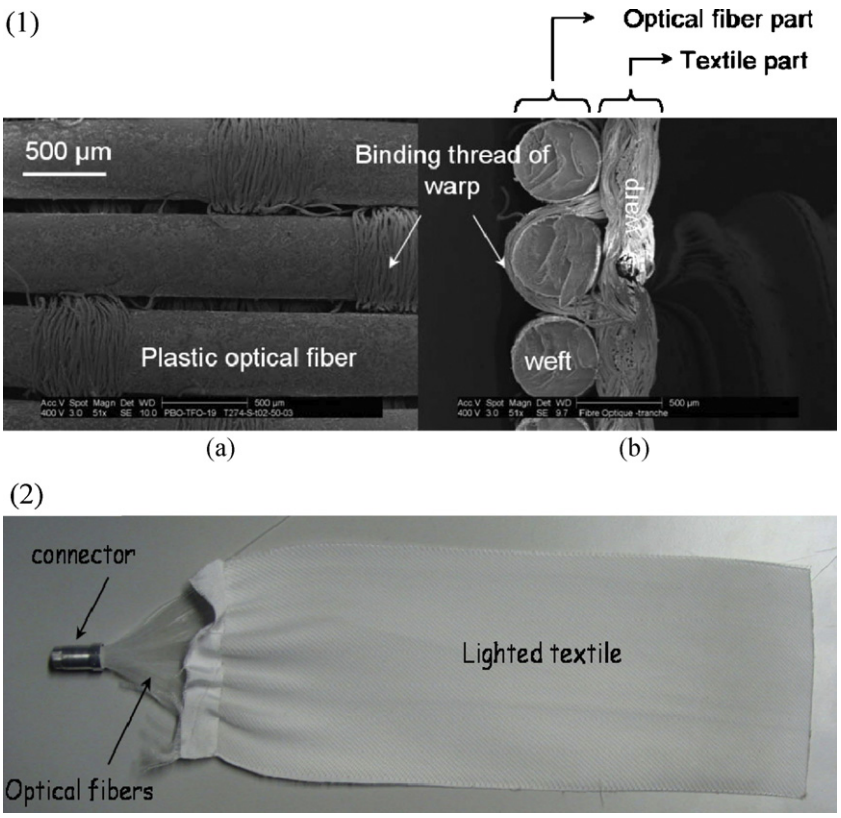

Fig. 1. SEM pictures of the textile (1a) planar view, (1b) sliced view and (2) a lighted textile sample.

the effect of the number of optical fibers on the efficiency. However, this kind of reactor has some limitations as the length because it appears an attenuation of the light with an optical fiber where the coating is made directly on the surface of the fiber.

In this paper, we present a new textile with polymeric optical fibers: plastic optical fiber (POF). First, the work has consisted in the structural characterization of the lighted textile and the adhesion of the catalyst. Then, the light distribution onto textile coated or not with photocatalyst is described. Finally, the photocatalytic efficiency for VOC degradation is demonstrated through formaldehyde degradation. This new technology, called Lightex® [24,25] has been developed by Brochier Technologies [26].

2. Experimental

2.1. Textile material

The textile is the combination of two parts: one is made in polymer textile (polyester) providing mechanical properties and one is composed with optical fibers. The plastic optical fibers (POF) have several advantages as being less expensive than glass/quartz optical fibers, flexible, resilient, tough, and resistant at temperature range from −55 °C to 70 °C [27]. They are fixed to the textile shape by binding weave following the Jacquard process meaning the interlacing, in a same plane, of fibers disposed in the direction of the chain (textile fiber) and some fibers disposed perpendicular to chain fibers, in the direction of the weft (optical fibers). These high-performance plastic optical fibers have a mean diameter of 500 μm. The optical fibers core is made in polymethyl methacrylate (PMMA) resin with a 480 μm mean diameter and covered with 10 μm of thick fluorinated polymer. All optical fibers for one textile sample are gathered to one extremity in an aluminum connector sealed with silicone. The optical fibers are linked with a binding thread as illustrated in Fig. 1.

2.2. Treatment of the material

Initially, light attenuation of fibers is 0.5 dB km^{-1} at λ equal to 380 nm. The patented treatment developed by Brochier Technologies [24,28] is a mechanical micro-texturation permitting a side emission of light along the optical fiber.

2.3. TiO_2 deposition

The photocatalyst used is TiO_2 Degussa P25. A bath of a concentrated aqueous suspension of TiO_2 (50 g L^{-1}) is maintained suspended with air lift. The coating was carried out by dipping the optical fiber textile in the bath maintained at 70 °C during 1 h. Then, the sample is dried during 2 h at 75 °C.

2.4. Analytical techniques

The morphological properties of the coated textile were obtained by combining several techniques.

2.4.1. Light emission

The first point is to understand the light emission from the fiber. The irradiance on the surface of each textile was recorded with sensor connected via optical fiber to a spectrometer Avaspec – 2048, equipped with a symmetrical Czerny-Turner design with 2048 pixel CCD detector array. The sensor allows collecting light on. The probe allows collecting light form half space thanks to a cosinus corrector, allowing to measure light coming from 2Π sr. To avoid the detector saturation, a diaphragm is added on the collection line. Before each measurement, the detector is calibrated with a calibration lamp AvaLight-DHS Deuterium-Halogen Light Sources. The

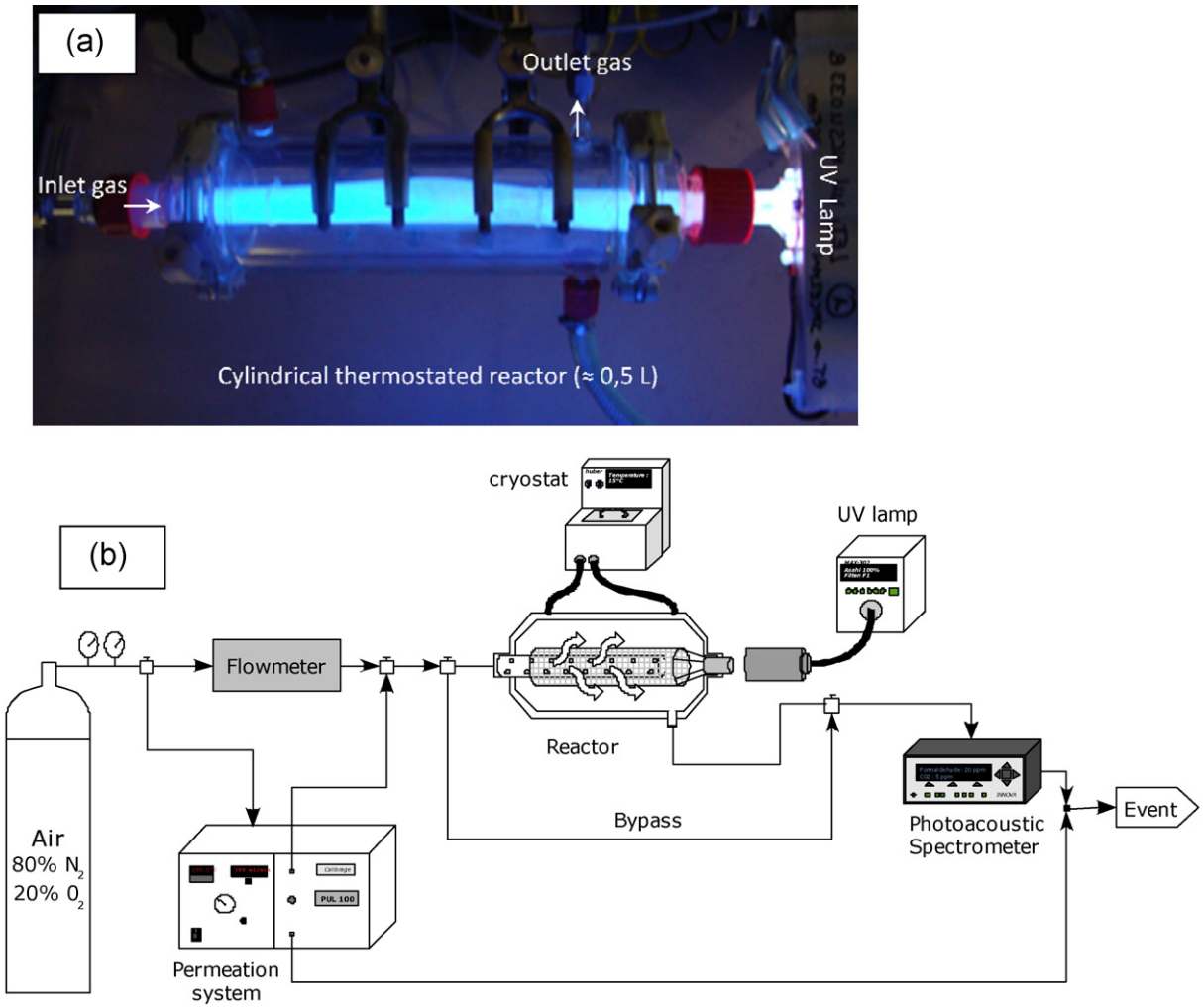

Fig. 2. (a) Picture of the photoreactor and (b) scheme of set up.

picture analyses are done using Panorama Studio Pro and GIMP softwares.

2.4.2. Surface structure

Optical microscopy (OM) with an open microscope BXFM with 3 objectives 10×, 50× and 100× from Jobin Yvon is used to determine the details of the surface texture. Environmental Scanning Electron Microscopy (ESEM) with a FEI XL30 ESEM FEG gives more information on the surface characterization. The rugosity of the surface is measured with (i) atomic force microscopy (AFM) with a Nanoscope III from Digital Instruments and with (ii) a microscope Axio Imager.M1m coupled with the software AxioVision.

2.4.3. Coating measurement

The quantification of Ti is obtained with a sample of 1 cm^2 dissolved in HF solution and analyzed with an ICP-AES "Activa" from Jobin Yvon.

2.4.4. TiO_2 repartition

The presence of TiO_2 on the optical fibers is revealed with Raman spectrometry using LabRam HR spectrometer coupled with an open microscope BXFM with 3 objectives 10×, 50× and 100× from Jobin Yvon. The mapping is obtained from 20 steps of 15 μm in *x*, and 20 steps of 17 μm in *y*. The size of the beam is 10 μm. The signal is measured during 40 s and the measurement is made two times to limit the noise and the aberration rays. The irradiant source is a laser Argon-Krypton fixed at 514 nm. The Raman cartography is done with a 2D motorized plate with a 0.1 μm path. The Raman spectrum acquisition is made with the LabSpec 4 software and the treatment of spectrum is done with LabSpec 5 software. Location of TiO_2 is completed with EDX-SEM techniques. The element cartographies are made with a FEI XL30 ESEM FEG.

2.4.5. TiO_2 adhesion

The adhesion of the photocatalyst is estimated by measuring the weight loss of the samples after a treatment under ventilation during 24 h. The air velocity is adjusted at 11 m s^{-1}.

2.5. Experimental apparatus and method

A new set-up was created for this new material (Fig. 2). It consisted in a cylindrical Pyrex reactor vessel of 530 ml included 2 inlets, one for the gas and one for the cap to fix the connector of the optical fiber. The reactor is thermostated at 15 °C thanks a double wall filled with water recirculating from a cryostat. In the reactor, the textile (240 cm^2) is rolled on a pierced tube which allows homogenizing the gas pollutants. The reactor is linked to a gas inlet. The textile is crossed by the air flow. Optical fibers are connected to a Xenon lamp from Asahi Spectra company. Prior to the photocatalytic tests, the photoreactor is flushed with air (100 mL min^{-1}) under illumination (λ > 290 nm) during 12 h to remove impurities. To generate the pollutant, a permeation system is used. Certified

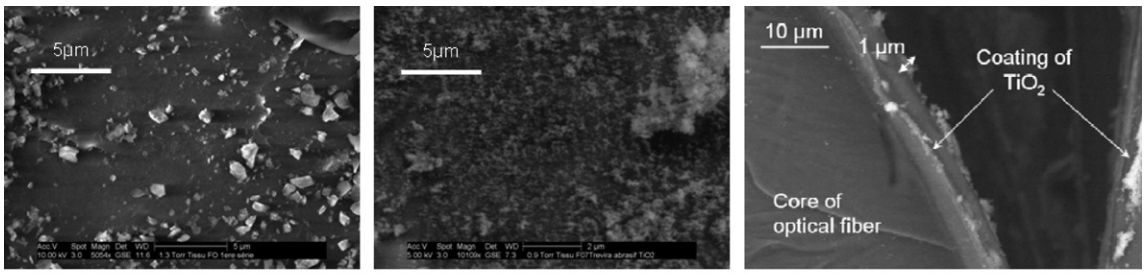

Fig. 3. ESEM pictures of textile treated: (a) without TiO_2 and (b) with TiO_2 (50 g L^{-1}) in planar view and (c) in sliced view.

permeation tubes used = are provided by Calibrage (France) or LNI (Switzerland) companies with permeation rates respectively of 3760 ng min^{-1} ± 7% and 3352 ng min^{-1} ± 5%.

The reactor is a one pass reactor and the flow rate used in this work was 0.1 L min^{-1}. A photoacoustic INNOVA 1213 spectrometer is connected on-line to the system to analyze the disappearance of formaldehyde and the formation of CO_2.

3. Results and discussion

3.1. Characterization of the textile after coating

3.1.1. Microscopy analysis of the photocatalyst deposition

The particles observed on the ESEM picture (Fig. 3a) result from some abrasive used for the mechanical treatment. Fig. 3b shows the coating of TiO_2. Even if the photocatalyst layer on fibers is not homogeneous on all the surface of textile, it completely seems to cover it. To measure the thickness of TiO_2, a sliced view of the optical fiber with TiO_2 coated is illustrated in Fig. 3c.

The TiO_2 layer thickness, measured by ESEM, is comprised between 1 and 3 µm. This deposition is similar to those obtained in the literature by Peill et al. [29], Wang and Ku [30], Choi et al. [18] or Danion et al. [20].

3.1.2. Repartition of photocatalyst

After TiO_2 deposition, Raman spectroscopy and EDX-SEM are used to visualize the repartition of TiO_2 on the optical fibers. On the left side of Fig. 4, is represented a micrography of a surface of 0.105 mm^2 (300 µm × 350 µm) of optical fiber and on the right side, the mapping obtained after analyses of Raman spectrum. On Raman spectrum (Fig. 4) is represented the presence of the three characteristic Raman shift peaks of TiO_2 anatase phase (393, 515 and 637 nm) and one characteristic Raman shift peak of the TiO_2 rutile phase (447 nm). They correspond to TiO_2 Degussa P25 which is a mixture of 80% of anatase phase and 20% of rutile phase. Part (a) in Fig. 4i is representative of the agglomerate of TiO_2 whereas on part (b) the amount of TiO_2 is negligible. However, it is important to note that in all cases a Raman signal is detected indicating that dip-coating of lighting textile allows to cover the overall optical fiber surface but does not form a homogeneous film. However, due to the geometry of optical fibers (cylindrical tube of 500 µm of diameter) and the absence of an automatic z focus on the Raman spectroscope,

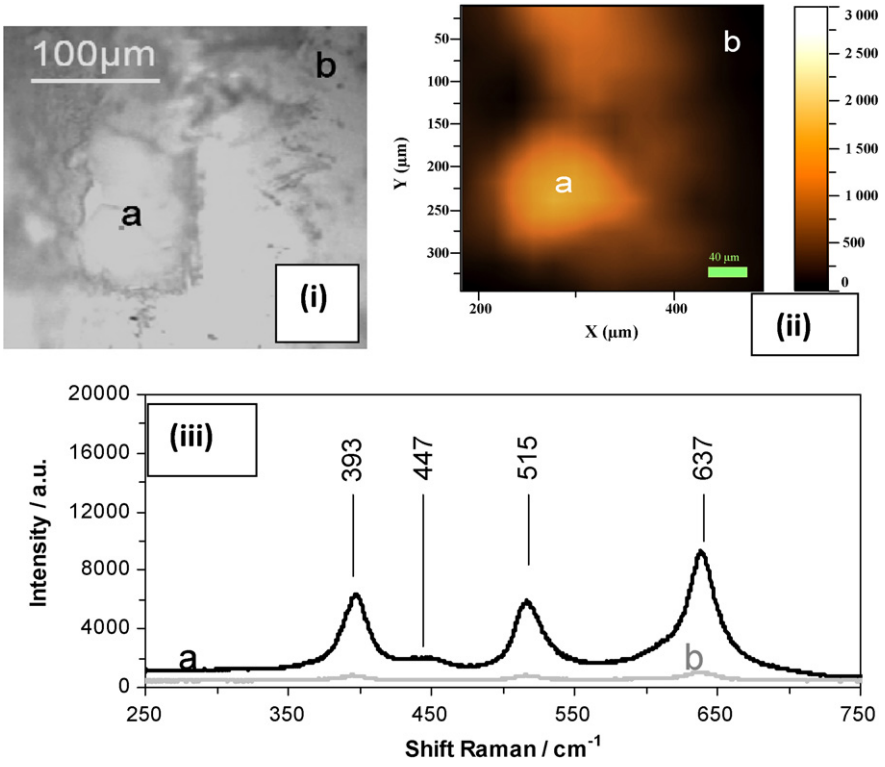

Fig. 4. Raman spectroscopy: (i) picture of analyzed zone, (ii) Raman cartography of zone, and (iii) Raman spectra of zone a and b.

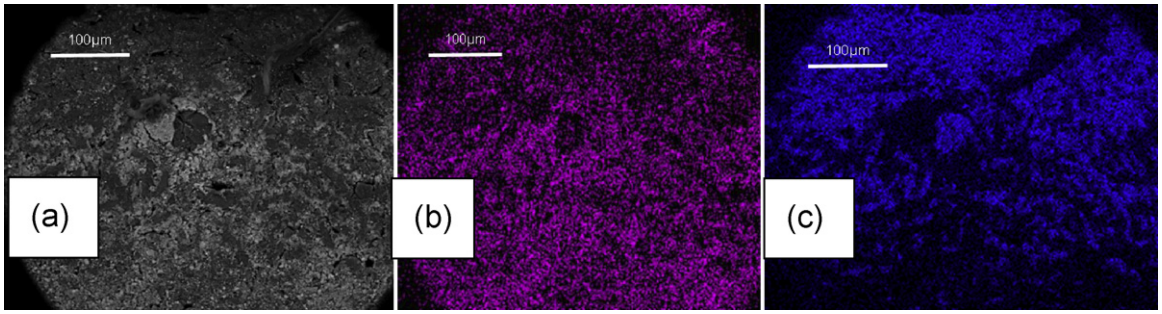

Fig. 5. (a) SEM picture of analyzed zone, (b) titanium cartography EDX and (c) fluor cartography EDX.

the analyzed zone is limited to the flat top of the fibers. EDX-SEM analysis has been performed (Fig. 5) to complete these results. SEM image and the corresponding Ti EDX-mapping obtained in various place of the textile show that the TiO_2 is dispersed on all lighting textile. Moreover mapping of fluor, an element of optical cladding (Fig. 5c) indicates that it is not present on all the optical fiber suggesting the perforation of optical cladding. The presence of fluor atoms is observed under TiO_2 layer due to the small thickness of photocatalyst film and the high electron beam power (10 kV).

3.1.3. Quantification and adhesion of photocatalyst

This new photocatalytic textile will be settled in Heating, Ventilating, and Air Conditioning (HVAC) systems. Consequently, it appears necessary to estimate the adhesion of photocatalyst under air flow found in HVAC. An air flow velocity of 11 m s^{-1}, at least two times greater than the one found in HVAC is used.

The quantity of TiO_2 fixed on the textile just after coating on a TiO_2 suspension of 50 g L^{-1} is around 5–6 g m^{-2}. However, textiles loose more than 60% of photocatalyst during the first 5 h before reaching a steady state (Fig. 6).

This result shows the need to condition the photocatalytic filters before using them in HVAC. However, it is important to notice that about 2 g m^{-2} of TiO_2 remains on the lighting textile. In our experimental conditions (0.025 m s^{-1}), no release of TiO_2 is observed.

3.2. Measurement of irradiance

3.2.1. Light losses

Our objective is to precisely characterize the losses of light of every part of the device to optimize the outlet of light at the level of the textile. So, firstly the spectrum of the lamp is measured in the domain of UVA (320–400 nm) with and without the connector. Secondly, the irradiance is measured with the beam of optical fibers and finally it is measured with lighted textile. The results are illustrated in Supplementary Fig. S1. About 11% of UV light is lost in the connector due to the Fresnel losses (reflexion at the interface air/fibers due to different indices) and to the lineic attenuation. 42% of UVA light is lost along the optical fibers after 30 cm by light scattering. In presence of lighted textile only 9% of UVA light is transmitted and the textile is able to spread 38% of the inlet light onto the textile surface.

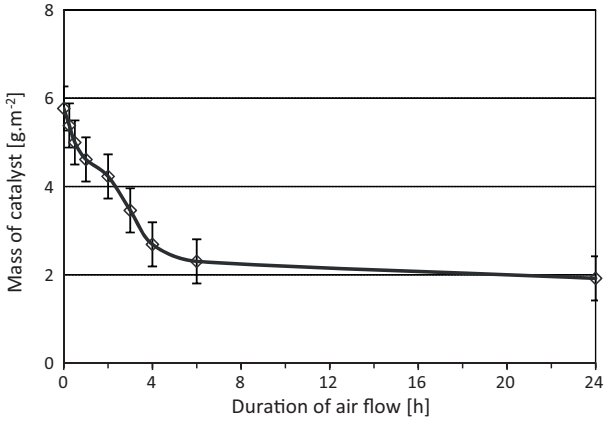

Fig. 6. Adhesion of photocatalyst under air flow as a function of time.

3.2.2. Light emission

To understand how the light is emitted, a study with different methods of microscopy is made. First, with optical microscopy (Fig. 7), a visible LED is connected to the textile and the surface is analyzed by an optical microscope. For a non treated textile, no light appears (Fig. 7a). For treated textile, dotted lights appear on the surface (Fig. 7c). For these both pictures (Fig. 7a and c), a zoom is made to see how the light is emitted from the surface of the optical fiber (Fig. 7b and d).

In Fig. 7, it can be observed that light is emitted from fiber from intense light sources or from large diffusive light surfaces.

There are two limitations for this study: the first one is the projection of the 3D fiber on a 2D picture. The second is the geometry of the optical fiber because the curvature limits the observation and deforms the dotted lights up and down of the picture where the surface goes out of the depth of field.

The comparison between photography of optical fiber with the surface roughness is made with optical microscopy and secondary electron microscopy on the same place. The SEM pictures show the defaults on the surface. For the same zone, the comparison between optical microscopy and SEM pictures is made in Fig. 8.

To show the effect of the treatment, a zoomed picture (Fig. 8c) is made on the defect (Fig. 8b).

For untreated fiber, the rugosity measured by AFM is 0.3 ± 0.1 µm. After the mechanical micro-textured treatment the rugosity reaches 10 ± 1 µm measured by SEM. Picture represented in Fig. 8 suggests that the intense light comes from the important modification of the thickness of the optical cladding.

The mechanical treatment partially destroys the optical cladding. The light can come out from the optical fiber because the rugosity changes the way the light is transported along fiber. This aspect of optical fiber was described by Endruweit et al. [31] and Harlin [32] who present two methods to get light emission from the side of the optical fiber. The first method is to modify the optical cladding with a mechanical process and the second one is the addition of elements which change the refractive index of the coating of optical fiber.

The light emission by mechanical micro-texturation of the cladding allows to obtain a relative homogeneity of the light distribution on the surface of the textile regarding the space resolution of the probe. If the light distribution is homogeneous for visible light because the visible probe surface area is 2 cm^2,

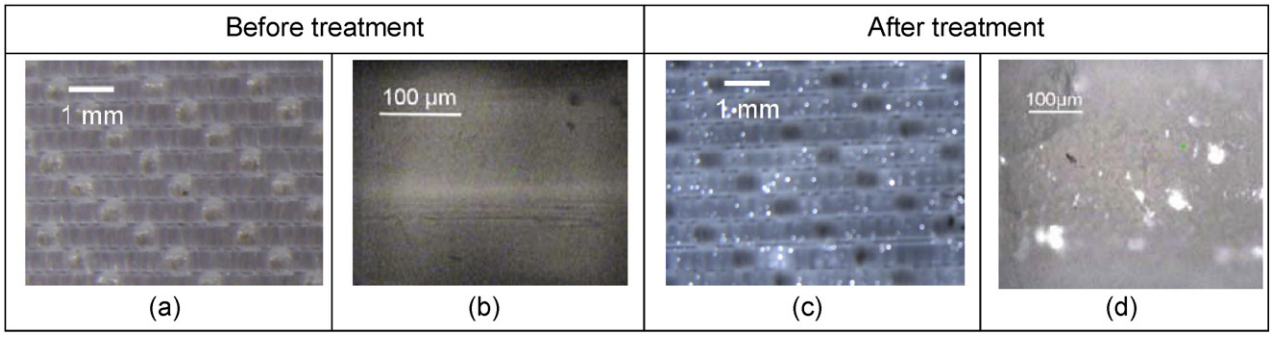

Fig. 7. Optical micrographs of the textile illuminated at different scale before and after the mechanical treatment.

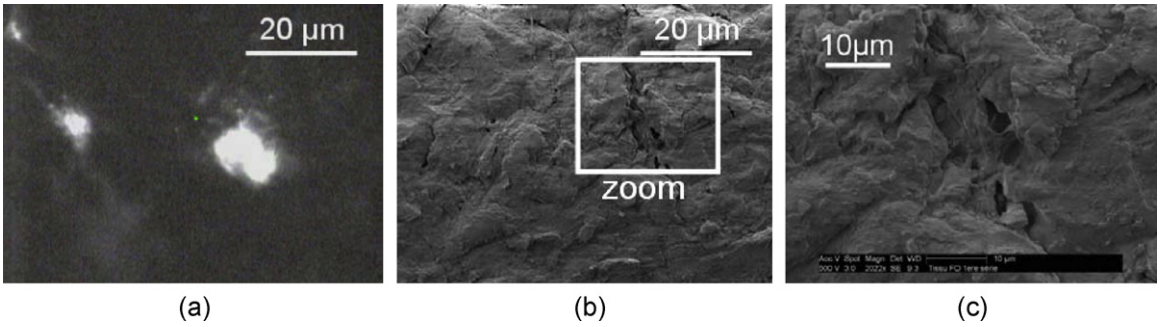

Fig. 8. Same surface as in Fig. 7 after treatment with (a) optical microscopy and (b and c) SEM picture.

for UV light, with a 4 mm^2 large probe, certain heterogeneity is observed.

3.2.3. Light emission modelling of the textile

As it was demonstrated previously, light is emitted from the textile by direct way or by diffusive way. The study is performed on a surface of 4 mm^2 including four optical fibers and two binding thread. To be representative of the sample surface, a series of 5 pictures in length and 7 pictures in width are taken as illustrated in Fig. 9. Then, the initial 35 pictures are gathered with the software Panorama studio Pro to obtain the picture in Fig. 9b. The structure of the textile corresponds to the initial structure. Then the code of each pixel is analyzed with GIMP software. The pixel codes are comprised in the range 0–255 with 0 corresponding to the black colour and 255 to the white colour. The pixel codes between 0 and 255 give the panel of gray scale.

The intense light appears with a white colour on the picture and is assumed to be characterized with codes in the range between 225 and 255. The gray part (linked to the diffuse light) is comprised between 120 and 225. The domain 0–120 corresponds to the binding point and the inter-optical fiber space with a colour near black.

First, photography of a 0.04 cm^2 zone of the treated textile without TiO_2 is done. There are 90,565 pixels corresponding to this surface. Among them 2261 pixels have code between 225 and 255 corresponding to 2% of global surface meaning that 0.08 mm^2 surface emits intense light. There are also 86,585 pixels with gray code between 120 and 225 corresponding to 95.3% of the surface with diffuse light emission. All these data are summarized in Table 1.

The extrapolation of this picture treatment to the whole textile area (300 cm^2) leads to obtain 6 cm^2 of intense light emission and 285.9 cm^2 of diffuse one.

Assuming that intense emission sources correspond to a mean radiant flux Φ_1 and diffuse emission sources correspond to a mean radiant flux Φ_2, the overall light emission Φ_{tot} is related to Φ_1 and Φ_2 and S_1 and S_2 by the relation:

$$\Phi_{tot}(S_1 + S_2) = \Phi_1 \times S_1 + \Phi_2 \times S_2 \quad (1)$$

with S_1 corresponding to the surface zone of bright light sources (pixel code from 225 to 255) and S_2 corresponding to the surface zone of diffuse light sources (pixel from 125 to 225).

The application of this relation to the 0.04 cm^2 zone for which the irradiance is 0.025 mW cm^2 and to the overall textile of 300 cm^2 for which the irradiance is 0.112 mW cm^2 gives the two following equations:

$$0.001 = 0.0008 \cdot \Phi_1 + 0.038 \cdot \Phi_2 \quad (2)$$

$$46 = 6 \cdot \Phi_1 + 286 \cdot \Phi_2 \quad (3)$$

Φ_1 is represented as a function of Φ_2, where Φ_1 is the intense flow and Φ_2 the diffuse flow (Fig. 10).

The ratio Φ_1/Φ_2 is superior to 1, so a major part of light is emitted via intense light sources comparative to the diffuse light. The treatment has to produce a lot of hole in the cover of the optical fiber to promote a lot of light on the surface of the lighted textile. The separation of the two curves is explained by the nonimportant inter optical fiber space for the sample size, so the size is over estimated.

Table 1
Experimental and calculated data for modeling of light emission in textile.

	Treated textile without TiO_2 coating
Size of sample (cm^2)	0.04
Number of pixels on the domain 0–255	90,565
Number of pixels on the domain 225–255	2261
Percent of surface with intense light	2.0%
Surface of intense light (cm^2)	0.0008
Number of pixels on the domain 120–225	86,585
Percent of surface with diffuse light	95.3%
Surface of diffuse light (cm^2)	0.038

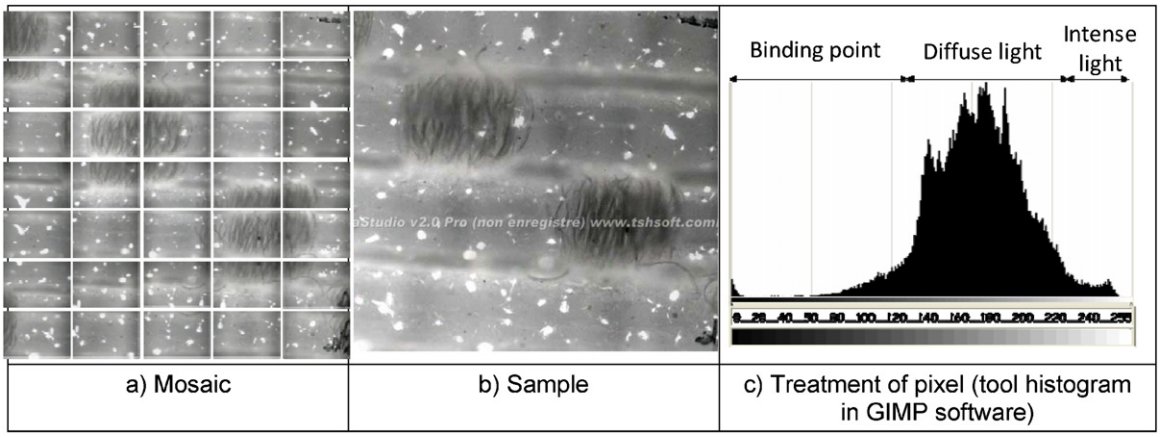

Fig. 9. Description of the treatment of the optical microscopy data: (a) mosaic of the 35 zones observed with optical microscopy, (b) reconstituted picture, and (c) distribution of color pixels from black to bright white.

3.2.4. Light absorption by the photocatalyst

The textile sample used for the light absorption study is constituted with optical fibers mixed with a textile nature in PE/PE. The light could be emitted sideway and the intensity of the irradiance flux has to be measured. A mapping of irradiance is made for each sample in order to estimate the homogeneity of the light emission. A pattern is used to measure the irradiance of each sample in the same conditions. The pattern for irradiance measurement includes regular holes of the size of the detector with five holes in the large and fifteen in the length. The mean value for each band in the width is done. A profile of irradiance in the panel 320–400 nm is obtained as a function of the textile length (Fig. 11).

For all textiles, the irradiance is almost constant on all the length. For a non treated textile, the irradiance is $7 \pm 2\,\mu W\,cm^{-2}$. For a treated textile the irradiance reaches $112 \pm 19\,\mu W\,cm^{-2}$. After the coating deposition, the irradiance is around $55 \pm 6\,\mu W\,cm^{-2}$. The system of irradiance measure takes into account the reflective part for each sample. So the difference of irradiance between the textile with TiO_2 and the one without TiO_2 corresponds to the light absorption by the photocatalyst and is around $58 \pm 19\,\mu W\,cm^{-2}$. If the catalyst is activated by UV light, it is able to promote photocatalytic oxidation.

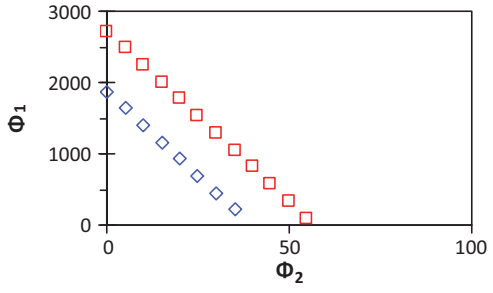

Fig. 10. Results of the modelling, □ Eq. (2), ◊ Eq. (3).

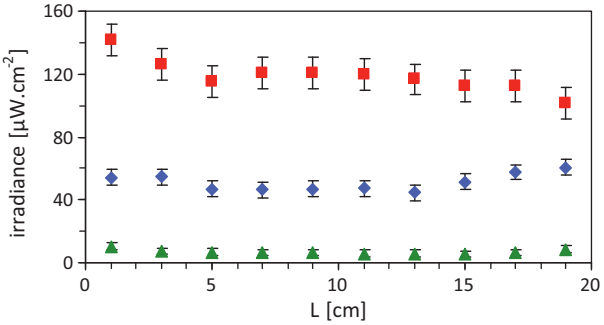

Fig. 11. Profile of irradiance measured in the range 320–400 nm on ▲ untreated textile; ■ treated textile; ◆ treated textile + TiO_2 at 50 g L^{-1}.

3.3. Photocatalytic degradation

Before starting the photocatalytic test, the sample was pretreated overnight under UV-irradiation with a Xenon lamp from Asahi Spectra (radiant flux $\Phi = 50\,mW\,cm^{-2}$ and $\lambda > 290\,nm$) and under dry air flow of $100\,ml\,min^{-1}$. The formaldehyde concentration ($1.5\,\mu mol\,L^{-1}$, equal to 35 ppm_v in air) was first stabilized and homogenized outside the reactor (step 1) before it was introduced in the reactor maintained in the dark (step 2). After reaching a steady state of formaldehyde concentration in the dark, the light was then switched on and maintained for 6 h (step 3) (Fig. 12).

The concentration of formaldehyde in presence of control textile or textile coating with TiO_2 maintained in the dark initially decreases when the polluted gas is sent through the reactor but it rapidly returns to its initial value. This decrease corresponds to the filling of the reactor by the gas flow but also the adsorption of formaldehyde on the textile. The difference of behavior with both textiles probably comes from their pressure loss difference. It is important to note that without mechanical treatment of optical fibers, no degradation is obtained.

Under UV-irradiation, the concentration of formaldehyde only decreases in presence of textile coating with TiO_2, putting in

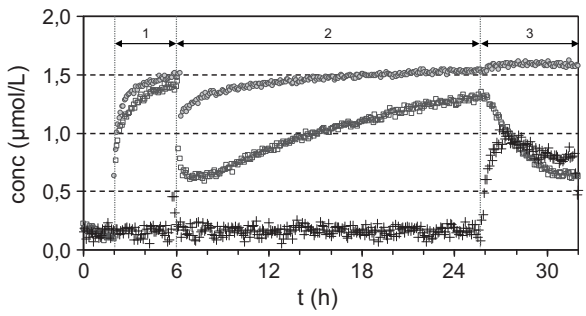

Fig. 12. Temporal changes in formaldehyde concentration during photocatalytic tests: ○ HCHO with textile without TiO_2; ■ HCHO with textile with TiO_2; + CO_2 with textile with TiO_2 (molar flow $D = 7.9\,\mu mol\,h^{-1}$; $D_{vol} = 0.1\,l\,min^{-1}$; UV radiant flux $\Phi = 50\,mW\,cm^{-2}$). Step 1 is by-passing reactor step, step 2 is dark step in the reactor, and step 3 is reaction step.

evidence the photocatalytic ability of this lighted textile to remove formaldehyde. Moreover, the formation of CO_2 is detected.

The formaldehyde degradation rate was determined under steady-state taken a mean value of 10 points and defined as the quantity of formaldehyde degraded per time unit and per unit of solid surface area, according to Eq. (4), where C_{in} is the mean value for the concentration in the reactor and C_{UV} is the mean value for the concentration after 6 h of illumination, D represents the volumic flow in $L\,h^{-1}$ and S the surface of textile.

$$r_{deg} = \frac{(C_{in} - C_{UV}) \times D}{S} \quad (4)$$

The degradation rate reaches $76\,\mu mol\,h^{-1}\,m^{-2}$ with a molar flow at $7.9\,\mu mol\,h^{-1}$, showing that this lighted textile coating with TiO_2 is efficient to remove pollution.

4. Conclusions

The ability of the textile constituted of optical fibers mechanically modified to allow radial leak of light has been demonstrated. The modelisation of the amount of light emitted on the surface of textile shows that major part of light is intense light. Diffuse light only represents around 2% of total emission. Finally, the textile is made photocatalytic by coating titanium dioxide on the surface. This new material integrating photocatalyst and light has demonstrated its efficiency to remove the formaldehyde, priority pollutant of indoor air.

Acknowledgments

This work was supported by the French National Research Agency (ANR PRECODD ANR-07-ECOT-009). The authors thank Francisco Cadete Santos Aires for the AFM measurement.

Appendix A. Supplementary data

Supplementary data associated with this article can be found, in the online version, at http://dx.doi.org/10.1016/j.apcatb.2012.03.033.

References

[1] P.L. Jenkins, T.J. Phillips, E.J. Mulberg, S.P. Hui, Atmospheric Environment Part A: General Topics 26 (12) (1992) 2141–2148.
[2] F. Grimaldi, A. Viala, Bulletin de l'académie nationale de médecine 191 (1) (2007) 21–33.
[3] H. Osawa, M. Hayashi, Building and Environment 44 (7) (2009) 1330–1336.
[4] C. Marchand, B. Buillot, S. Le Calve, P. Mirabel, Atmospheric Environment 40 (7) (2006) 1336–1345.
[5] I.K. Koponen, A. Asmi, P. Keronen, K. Puhto, M. Kulmala, Atmospheric Environment 35 (8) (2001) 1465–1477.
[6] M.R. Hoffmann, S.T. Martin, W.Y. Choi, D.W. Bahnemann, Chemical Reviews 95 (1) (1995) 69–96.
[7] T. Noguchi, A. Fujishima, Environmental Science & Technology 32 (23) (1998) 3831–3833.
[8] A. Fujishima, X.T. Zhang, D.A. Tryk, Surface Science Reports 63 (12) (2008) 515–582.
[9] J.M. Herrmann, C. Duchamp, M. Karkmaz, B.T. Hoai, H. Lachheb, E. Puzenat, C. Guillard, Journal of Hazardous Materials 146 (3) (2007) 624–629.
[10] J. Zhao, X.D. Yang, Building and Environment 38 (5) (2003) 645–654.
[11] N.J. Peill, M.R. Hoffmann, Environmental Science & Technology 29 (12) (1995) 2974–2981.
[12] R.D. Sun, A. Nakajima, I. Watanabe, T. Watanabe, K. Hashimoto, Journal of Photochemistry and Photobiology A: Chemistry 136 (1–2) (2000) 111–116.
[13] R.Q. Tan, Y. He, Y.F. Zhu, B.Q. Xu, L.L. Cao, Journal of Materials Science 38 (19) (2003) 3973–3978.
[14] T. Yuranova, D. Laub, J. Kiwi, Catalysis Today 122 (1–2) (2007) 109–117.
[15] R.E. Marinangeli, D.F. Ollis, AIChE Journal 23 (4) (1977) 415–426.
[16] R.E. Marinangeli, D.F. Ollis, AIChE Journal 26 (6) (1980) 1000–1008.
[17] K. Hofstadler, R. Bauer, S. Novalic, G. Heisler, Environmental Science & Technology 28 (4) (1994) 670–674.
[18] W. Choi, J.Y. Ko, H. Park, J.S. Chung, Applied Catalysis B: Environmental 31 (3) (2001) 209–220.
[19] H. Joo, H. Jeong, M. Jeon, I. Moon, Solar Energy Materials and Solar Cells 79 (1) (2003) 93–101.
[20] A. Danion, J. Disdier, C. Guillard, F. Abdelmalek, N. Jaffrezic-Renault, Applied Catalysis B: Environmental 52 (3) (2004) 213–223.
[21] A. Danion, C. Bordes, J. Disdier, J.-Y. Gauvrit, C. Guillard, P. Lanteri, N. Jaffrezic-Renault, Journal of Photochemistry and Photobiology A: Chemistry 168 (3) (2004) 161–167.
[22] A. Danion, J. Disdier, C. Guillard, O. Paisse, N. Jaffrezic-Renault, Applied Catalysis B: Environmental 62 (2006) 274–281.
[23] A. Danion, J. Disdier, C. Guillard, N. Jaffrezic-Renault, Journal of Photochemistry and Photobiology A: Chemistry 190 (2007) 135–140.
[24] C. Brochier, D. Malhomme, E. Deflin - Brevet 2007. « Nappe textile présentant des propriétés dépolluantes par photocatalyse » - n° de délivrance FR2910341, 2008-06-27 (A1) et FR2910341, 2009-02-06 (B1). http://fr.espacenet.com/publicationDetails/originalDocument?CC=FR&NR=2910341A1&KC=A1&FT=D&date=20080627&DB=fr.espacenet.com&locale=fr_FR.
[25] C. Brochier, E. Deflin, T. Breting - Brevet N° WO 2008/061789, Complexe éclairant. 2008. « Complexe éclairant comportant une source lumineuse présentant une nappe de fibres optiques » - FR2907194 (A1) 2008-04-18 et FR2907194 (B1) - 2010-08-27. http://fr.espacenet.com/publicationDetails/biblio?DB=fr.espacenet.com&adjacent=true&locale=fr_FR&FT=D&date=20080418&CC=FR&NR=2907194A1&KC=A1.
[26] SARL, C.B. S. www.brochiertechnologies.com.
[27] Mitsubishi CK-20. http://www.i-fiberoptics.com/pdf/CK20.pdf.
[28] C. Brochier, E. Deflin - Brevet N° WO 2008/062141, Complexe éclairant verrier. 2008. FR2908864 (A1) - 2008-0523. http://fr.espacenet.com/publicationDetails/biblio?DB=fr.espacenet.com&adjacent=true&locale=fr_FR&FT=D&date=20080523&CC=FR&NR=2908864A1&KC=A1.
[29] N.J. Peill, M.R. Hoffmann, Environmental Science & Technology 30 (9) (1996) 2806–2812.
[30] W. Wang, Y. Ku, Chemosphere 50 (8) (2003) 999–1006.
[31] A. Endruweit, A.D. Alobaidani, D. Furniss, A.B. Seddon, T. Benson, M.S. Johnson, A.C. Long, Optics and Lasers in Engineering 46 (2008) 97–105.
[32] A. Harlin, AUTEX Research Journal 3 (1) (2003).